DOI: 10.1002/ejic.200700582

Divalent Nickel, Cobalt and Iron Complexes of an Amide-Appended N_2S_2 Ligand: Synthesis, Characterization and Reactivity with Hydroxide Anion

Gajendrasingh K. Ingle,[a] Magdalena M. Makowska-Grzyka,[a] Atta M. Arif,[b] and Lisa M. Berreau*[a]

Keywords: N,S ligands / Amides / Metal effects / Deprotonation

Divalent nickel, cobalt and iron complexes {[(bmppa)-Ni(CH_3CN)](ClO_4)$_2$ (**1**), [(bmppa)Co(CH_3CN)](ClO_4)$_2$ (**2**), [(bmppa)Fe(CH_3CN)](ClO_4)$_2$ (**3**)} of an amide-appended N_2S_2-donor ligand {bmppa = *N*,*N*-bis(2-methylthio)ethyl-*N*-[(6-pivaloylamido-2-pyridyl)methyl]amine} have been prepared and characterized using ^{1}H NMR, IR, UV/Vis, elemental analysis and magnetic moment measurements. The complexes **2** and **3** were also characterized by X-ray crystallography. When treated with 1 equiv. of $Me_4NOH{\cdot}5H_2O$ in methanol, **1** and **2** form deprotonated amide complexes {[(bmppa$^-$)Ni]ClO_4 (**4**), [(bmppa$^-$)Co]$ClO_4{\cdot}H_2O$ (**5**)} which were isolated and characterized by ^{1}H NMR, IR, UV/Vis, elemental analysis and magnetic moment measurements. Treatment of the Fe^{II} complex **3** with 1 equiv. of $Me_4NOH{\cdot}5H_2O$ in methanol produced the free bmppa chelate ligand and a precipitate of an unidentified iron species. Heating of **5** at 50 °C in methanol for 5 d resulted in a ca. 50 % yield of amide methanolysis products and a small amount of products resulting from oxidative *N*-dealkylation of the bmppa ligand. It has been previously shown that a zinc analog of **5** undergoes quantitative amide methanolysis under milder conditions. Complex **4** does not undergo amide cleavage upon heating at 50 °C in methanol for 5 d. A rationale for the metal-dependent amide methanolysis reactivity of these complexes is proposed on the basis of structural differences in the "parent" protonated complexes.

Introduction

Amide cleavage reactions are catalyzed by a variety of metal-containing enzymes. An amide hydrolase that has received considerable recent attention is peptide deformylase (PDF). In the active site of PDF, a nitrogen/sulfur-ligated iron(II) center is involved in the hydrolysis of a formamide moiety during polypeptide biosynthesis.[1–4] Notably, replacement of the Fe^{II} ion with Ni^{II} and Co^{II} produces catalytically active enzyme.[2,3,5–8] However, with Zn^{II} as the active-site metal ion, the enzyme activity is reduced by ca. 100-fold.[7,9]

To investigate the role of the metal center in PDF enzymes, Goldberg and co-workers have investigated the structural and spectroscopic properties of synthetic complexes of relevance to resting state and formato-bound forms of the enzyme.[10–14] These complexes are supported by an N_2S(thiolate) ligand {PATH = 2-methyl-1-[methyl(2-pyridin-2-ylethyl)amino]propane-2-thiolate}. A zinc hydroxide complex of the PATH ligand has been shown to promote the hydrolysis of phosphate and carboxy esters;[12,13] however, no reactivity with an amide substrate has been reported.

We recently reported studies of the formyl ester and formamide cleavage reactivity of a Zn^{II}–OH complex, [(bmnpaZn)$_2$(μ-OH)$_2$](ClO_4)$_2$, supported by an N_2S_2 ligand containing an internal hydrogen-bond donor.[15] In acetonitrile, this complex promotes the hydrolysis of methyl formate to produce methanol and a (formato)zinc complex {[(bmnpa)Zn(O_2CH)]ClO_4}. In methanol, the (hydroxido)-zinc complex reacts with the alcohol to produce a (methoxido)zinc complex. Treatment of this Zn–OMe complex with formanilide results in the formation of aniline, methyl formate, and [(bmnpa)Zn(O_2CH)]ClO_4. The formation of both methyl formate and the (formato)zinc complex indicated that both methanolysis and hydrolysis reactions occur in the reaction mixture.

Recently, we investigated in detail the amide methanolysis reactivity of zinc complexes of amide-appended N_4, N_3S, and N_2S_2 donor ligands in the presence of hydroxide anion in methanol.[16–18] The reaction pathway for amide cleavage in these systems was found to involve the initial formation of a (deprotonated amide)zinc complex which subsequently undergoes reaction with methanol to produce a reactive complex for amide methanolysis. The products generated in these amide methanolysis reactions

[a] Department of Chemistry and Biochemistry, Utah State University,
0300 Old Main Hill, Logan, UT 84322-0300, USA
Fax: +1-435-797-3390
E-mail: berreau@cc.usu.edu
[b] Department of Chemistry, University of Utah,
315 S. 1400 E., Salt Lake City, UT, 84112-0850, USA

are a zinc complex of a primary amine-appended chelate ligand, methyl trimethylacetate, and 1 equiv. of Me_4NClO_4.[16–18]

The research described herein examines how the amide methanolysis reactivity of divalent metal complexes of an amide-appended N_2S_2 ligand is influenced by the nature of the metal center. This work has some relevance to peptide deformylase, as we have examined the structural, spectroscopic, and amide cleavage reactivity properties of Ni^{II}, Co^{II}, and Fe^{II} analogs of $[(bmppa)Zn](ClO_4)_2$ {bmppa = *N*,*N*-bis(2-methylthio)ethyl-*N*-[(6-pivaloylamido-2-pyridyl)-methyl]amine}.[16,18] To the best of our knowledge, this is the first direct comparison of amide cleavage reactivity in structurally related complexes of these metal ions. Findings of this study include: (1) similar to the chemistry of $[(bmppa)Zn](ClO_4)_2$, the Ni^{II} and Co^{II} analogs form deprotonated amide complexes upon treatment with hydroxide anion, whereas the Fe^{II} analog decomposes to yield free bmppa ligand and unidentified iron species; and (2) of the non-zinc metals only the (deprotonated amide)Co^{II} complex reacts with methanol to yield amide methanolysis products, albeit in lower yield than the zinc analog. A rationale for the metal-dependent amide methanolysis reactivity of these complexes is proposed on the basis of structural differences in the "parent" protonated complexes.

Results and Discussion

Synthesis and Characterization of Divalent Metal Complexes

Mononuclear divalent nickel, cobalt, and iron complexes of the bmppa ligand were prepared by treatment of the ligand with $[M(H_2O)_6](ClO_4)_2$ (M = Ni, Co, and Fe) in methanol. Recrystallization of the resulting metal complex from acetonitrile-containing solutions resulted in the isolation of $[(bmppa)M(CH_3CN)](ClO_4)_2$ (**1**: M = Ni^{II}; **2**: M = Co^{II}; **3**: M = Fe^{II}; Scheme 1). Each complex has been characterized by elemental analysis, ^1H NMR, FTIR, UV/Vis spectroscopy, mass spectrometry, and a magnetic moment measurement. For **2** and **3**, crystals suitable for single-crystal X-ray diffraction were obtained.

ORTEP drawings of the cationic portions of the X-ray structures of **2** and **3** are shown in Figure 1. Selected bond lengths and angles are given in Table 1. These complexes are nearly isostructural, with both crystallizing in the $P2_1/c$ space group. In each the divalent metal center is ligated by all of the available donor atoms of the chelate ligand and one acetonitrile solvent molecule. The geometry of the metal center in these complexes is distorted octahedral with the acetonitrile molecule positioned in the same plane as the chelate ring containing the amide moiety, thereby bisecting the S(1)–M–S(2) angle. In comparing **2** and **3**, the average M–S (**2**: 2.50 Å; **3**: 2.33 Å) and M–N (**2**: 2.10 Å; **3**: 1.99 Å) bonds are notably longer in the Co^{II} derivative, whereas the M–O(1) distances differ by only ca. 0.06 Å [**2**: Co–O(1) 2.0125(15) Å; **3**: Fe–O(1) 1.956(2) Å].

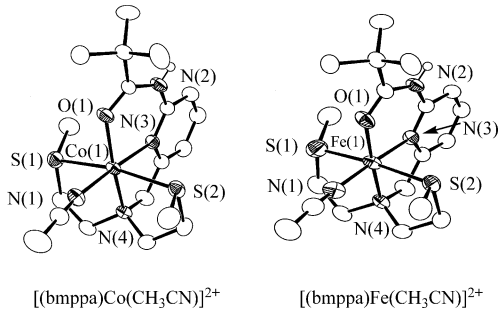

Figure 1. ORTEP drawings of the cationic portions of **2** (left) and **3** (right). Ellipsoids are plotted at the 50% probability level. All hydrogen atoms except the amide proton are not shown for clarity.

The solid-state FTIR spectral features of **1**–**3** in KBr are consistent with amide coordination. Specifically, the amide C–O stretching vibration is shifted to lower energy (ca. 1648–1633 cm^{-1}) as compared to the position of this vibration in the free bmppa ligand (1687 cm^{-1}). Solution IR spectra of **1**–**3** in acetonitrile (100 mM) have features in the region of 1700–1550 cm^{-1} that are very similar to the solid-state spectra, providing evidence that amide coordination is maintained in solution. In the solid-state FTIR spectra, each complex exhibits a ν_{N-H} stretching vibration at ca. 3350–3300 cm^{-1}. The solution UV/Vis absorption spectral features of **1**–**3** are summarized in Table 2. All complexes show strong ligand-based absorptions at <400 nm. For **2**, a 511 nm (ε = 44 $M^{-1}cm^{-1}$) transition is consistent with the Co^{II} center having a six-coordinate pseudo-octahedral geometry in solution.[19] Each complex contains a high-spin pseudo-octahedral metal center, as evidenced by solution

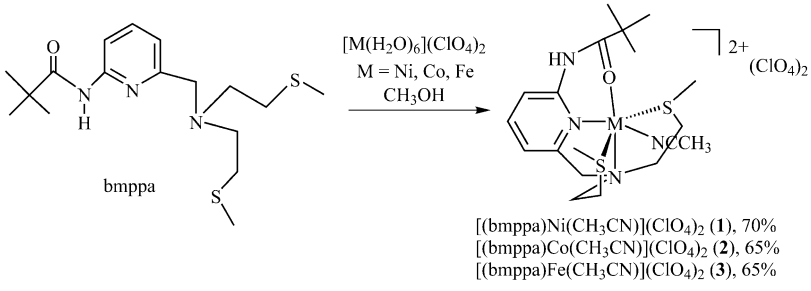

Scheme 1. Synthetic route for the preparation of divalent metal complexes of the bmppa ligand.

Table 1. Selected bond lengths and angles.[a]

	2	3
M(1)–O(1)	2.0125(15)	1.956(2)
M(1)–N(1)	2.0667(19)	1.957(3)
M(1)–N(3)	2.0980(17)	1.976(2)
M(1)–N(4)	2.1369(18)	2.050(3)
M(1)–S(1)	2.5092(7)	2.3195(12)
M(1)–S(2)	2.4226(7)	2.3395(10)
O(1)–M(1)–N(1)	94.42(7)	89.95(11)
O(1)–M(1)–N(3)	86.00(7)	90.52(10)
N(1)–M(1)–N(3)	175.08(8)	177.01(12)
O(1)–M(1)–N(4)	164.86(7)	174.49(10)
N(1)–M(1)–N(4)	99.06(7)	95.21(11)
N(3)–M(1)–N(4)	81.15(7)	84.42(10)
O(1)–M(1)–S(1)	90.71(5)	92.01(8)
N(1)–M(1)–S(1)	87.16(6)	87.65(9)
N(3)–M(1)–S(1)	97.73(5)	95.28(8)
N(4)–M(1)–S(1)	83.15(5)	86.31(8)
O(1)–M(1)–S(2)	99.93(5)	94.28(8)
N(1)–M(1)–S(2)	91.76(6)	91.36(9)
N(3)–M(1)–S(2)	83.34(5)	85.66(8)
N(4)–M(1)–S(2)	86.57(5)	87.52(8)
S(1)–M(1)–S(2)	169.36(2)	173.63(4)

[a] Estimated standard deviation in the last significant figure is given in parentheses.

magnetic moment measurements performed at 298 K using the Evans method.[20] For **1**–**3** the effective magnetic moment is higher than the spin-only value (Ni^{II}: 2.8 μ_B; Co^{II}: 3.9 μ_B; Fe^{II}: 4.9 μ_B) calculated for the high-spin metal center due to spin-orbit coupling.[21]

Table 2. Selected properties of **1**–**3**.

	1	2	3
UV/Vis: λ [nm] (ε [$M^{-1}cm^{-1}$])[a]	536 (14), 867 (40), 953 (40)	511 (44)	754 (10)
μ_{eff} [μ_B]	3.0	4.6	5.0

[a] Spectra collected in CH_3CN.

Complexes **1**–**3** exhibit paramagnetically shifted ^1H NMR spectra. These spectra are shown in Figures 2, 3, and 4 to illustrate that each complex exhibits signals that can be identified on the basis of integrated intensity, deuterium substitution, and/or ^1H-^1H COSY experiments. When dissolved in CD_3CN, complex **1** (Figure 2) exhibits a *tert*-butyl methyl signal at δ = 4.6 ppm and an amide proton resonance at $\delta \approx -6$ ppm, the latter of which was assigned by deuterium substitution (with D_2O). In the region of $\delta \approx$ 180–10 ppm are several resonances. A sharp signal at δ = 14.2 ppm has been tentatively assigned as the γ-H of the pyridyl ring. While the remaining signals have not been conclusively assigned, we believe that the signals at $\delta \approx$ 49 and 73 ppm are for the β-H atoms of the pyridyl ring. For **2** in CD_3CN (Figure 3), the *tert*-butyl methyl signal is found at $\delta \approx$ 28 ppm. The β-H and γ-H signals for this complex have been assigned on the basis of a ^1H-^1H COSY spectrum. Addition of D_2O to a solution of **2** in CD_3CN failed to reveal the signal of the amide hydrogen atom (by loss of the ^1H signal). When dissolved in CD_3CN, complex **3** (Figure 4) exhibits resonances in the range of $\delta \approx$ 110–0 ppm. The *tert*-butyl methyl resonance of **3** is found at δ = 4.2 ppm in dry CD_3CN. We tentatively assigned the β-H and γ-H signals for this complex as shown in Figure 4 on the basis of peak width and intensity. The ^1H NMR features of this complex exhibit a solvent dependence, with addition of a small amount of D_2O (2 μL) to a water-free CD_3CN solution of **3** producing an upfield shift of the *tert*-butyl resonance to $\delta \approx$ 3.4 ppm. The addition of D_2O also produces changes in the spectrum in the region of δ = 20–30 ppm. Analysis of the ^1H NMR features of **3** as a function of solvent remains under investigation.

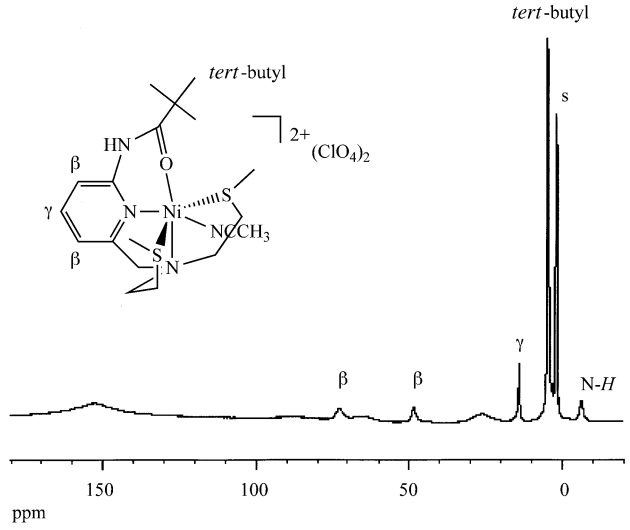

Figure 2. ^1H NMR spectrum of **1** in dry CD_3CN at ambient temperature (s = signal of CD_2HCN).

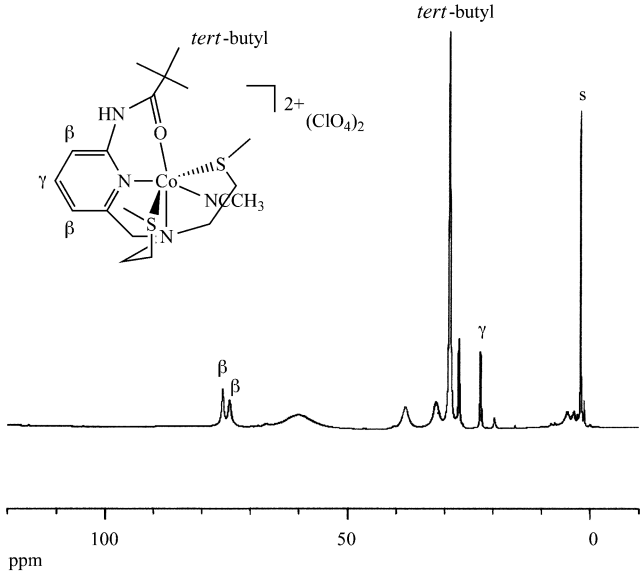

Figure 3. ^1H NMR spectrum of **2** in dry CD_3CN at ambient temperature (s = signal of CD_2HCN).

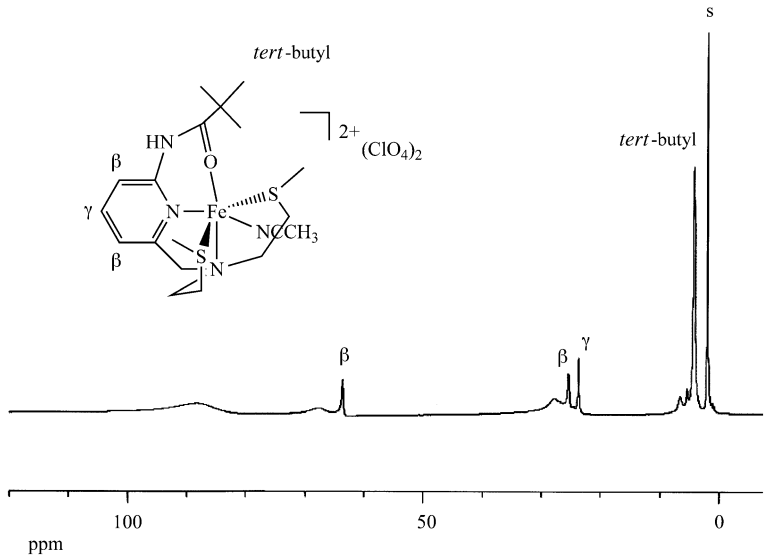

Figure 4. ^{1}H NMR spectrum of **3** in dry CD_3CN at ambient temperature (s = signal of CD_2HCN).

Reactivity of 1–3 with Hydroxide Anion in Methanol – Isolation of Deprotonated Amide Complexes

We have previously reported that treatment of [(bmppa)Zn]$(ClO_4)_2$ with $Me_4NOH{\cdot}5H_2O$ in methanol-containing solutions results in amide methanolysis.[16,18] This reaction proceeds through the initial formation of a depronated amide complex, [(bmppa$^-$)Zn]ClO_4, which subsequently undergoes reaction with methanol to produce the reactive species for amide cleavage.[18] Treatment of **1** with $Me_4NOH{\cdot}5H_2O$ in methanol results in the formation of the deprotonated amide complex [(bmppa$^-$)Ni]ClO_4 (**4**, Scheme 2) which has been isolated and characterized by elemental analysis, FTIR, UV/Vis, ^{1}H NMR spectroscopy, and a solution magnetic moment measurement. The elemental analysis data for **4** is best fit with one perchlorate anion and no coordinated solvent molecules, suggesting an overall coordination number of five for the Ni^{II} center. The FTIR spectrum of **4** differs from that of [(bmppa)Ni$(CH_3CN)](ClO_4)_2$ (**1**) in that intense vibrations found in the region of ca. 1600–1635 cm^{-1} for **1**, which include the $\nu(CO_{amide})$ vibration, are not present in the spectrum of **4**. Instead, a series of intense new vibrations is centered at ca. 1450 cm^{-1}, which is consistent with the presence of a deprotonated amide moiety.[17] The UV/Vis absorption spectral features and solution magnetic moment of **4** are given in Table 3. The absorption and ^{1}H NMR (Figure 5) spectral features of **4** are different from those of **1**. In the ^{1}H NMR spectrum of **4** no signal upfield of zero is present, consistent with amide deprotonation. Two prominent resonances at $\delta \approx 49$ and 73 ppm in the spectrum of **1** appear to have shifted to $\delta \approx 61$ and 64 ppm in **4**. These resonances are assigned to the β-H atoms of the pyridyl ring. It is important to note that resonance structures for the deprotonated amide moiety can be drawn wherein the anionic charge is positioned at the β-carbon atoms of the pyridyl ring, thus providing a rational for why the β-H signals shift upon deprotonation.[17] The *tert*-butyl methyl signal of **4** is shifted slightly downfield (δ = 5.6 ppm) relative to the position of the same signal of **1** (δ = 4.6 ppm). The γ-H resonances of **1** and **4** are at nearly identical chemical shifts (δ = 14.2 ppm).

Table 3. Selected properties of **4** and **5**.

	4	**5**
UV/Vis: λ [nm] (ε [$M^{-1}cm^{-1}$])[a]	530 (20), 835 (20), 1034 (35)	548 (140)
μ_{eff} [μ_B]	3.1	3.7

[a] Spectra collected in CH_3CN.

Treatment of [(bmppa)Co$(CH_3CN)](ClO_4)_2$ (**2**) with $Me_4NOH{\cdot}5H_2O$ results in the formation of a brown deprotonated amide complex, [(bmppa$^-$)Co]$ClO_4{\cdot}H_2O$ (**5**). The elemental analysis of **5** is best fit with the inclusion of one water molecule in the bulk, isolated sample of the com-

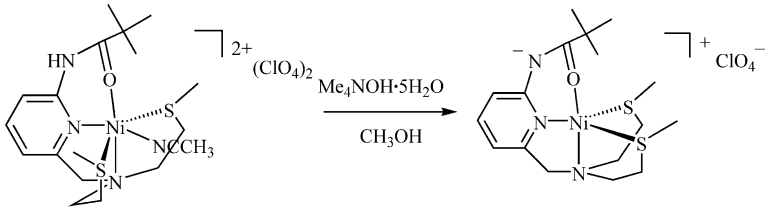

[(bmppa)Ni$(CH_3CN)](ClO_4)_2$ (**1**) [(bmppa$^-$)Ni]ClO_4 (**4**)

Scheme 2. Reaction of **1** with $Me_4NOH{\cdot}5H_2O$.

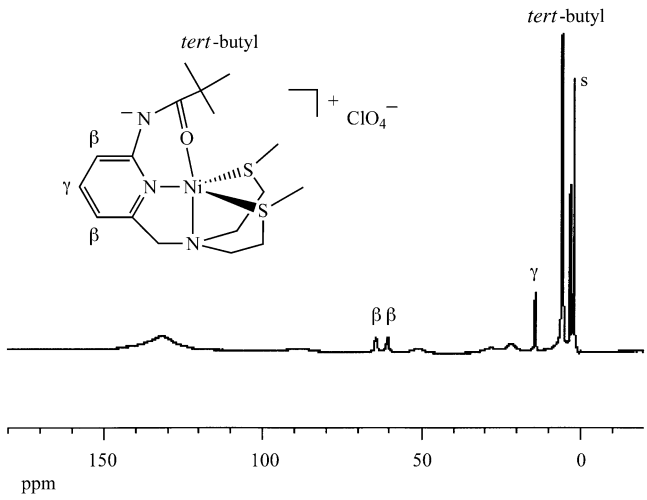

Figure 5. ^{1}H NMR spectrum of **4** in dry CD_3CN at ambient temperature (s = signal of CD_2HCN).

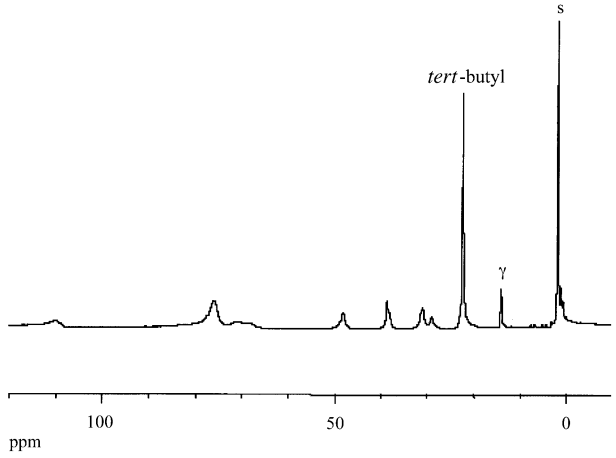

Figure 6. ^{1}H NMR spectrum of **5** in dry CD_3CN at ambient temperature (s = signal of CD_2HCN).

pound. Additional evidence for the presence of this water molecule comes from FTIR spectroscopic analysis of a crystalline sample of the complex, which revealed a ν_{O-H} vibration at 3430 cm^{-1}. Also present in the FTIR spectrum of **5** is an intense set of vibrations at ca. 1450 cm^{-1}, which is characteristic of the presence of a deprotonated amide moiety.[17] The UV/Vis absorption spectrum of **5** includes a d–d transition at 548 nm (ε = 140 $M^{-1}cm^{-1}$). The intensity of this absorption band is consistent with the Co^{II} center having a coordination number of five in acetonitrile.[19] On the basis of this spectroscopic data, we propose that the Co^{II} center in **5** is ligated by the five available donors in the deprotonated bmppa$^-$ ligand and that the water molecule is not coordinated to the metal center. The difference in coordination number between **5** and **2** may be the reason why the ^{1}H NMR features of **5** (Figure 6) are noticeably different from those of its protonated analog (Figure 3). Specifically, whereas **5** has resonances over a ca. 120 ppm region, the parent complex **2** has signals over a ca. 80 ppm region. Overall, the deprotonated amide complex exhibits generally sharper signals. In terms of specific resonances, complex **5** has a *tert*-butyl methyl resonance at $\delta \approx 22$ ppm whereas for **2** this signal is found at δ = 29 ppm. Similarly, **5** exhibits a γ-H resonance (δ = 14.2 ppm) upfield of where this signal appears in the ^{1}H NMR spectrum of **2** (δ = 22.0 ppm). The magnetic moment for **5** (μ_{eff} = 3.7 μ_B) is slightly below the spin-only value calculated for three unpaired electrons (μ_{eff} = 3.87 μ_B). Thus far, efforts to generate X-ray quality crystals of **5** have failed, with only microcrystalline solids being isolated.

Treatment of the Fe^{II} complex [(bmppa)Fe(CH$_3$CN)](ClO$_4$)$_2$ (**3**) with $Me_4NOH{\cdot}5H_2O$ in methanol under nitrogen results in the formation of a dark green precipitate in a yellow solution. Physical separation of the precipitate and the soluble components, followed by removal of the solvent from the soluble portion, yielded the free bmppa ligand in 78% yield. The green precipitate was dried under vacuum and analyzed by IR spectroscopy. This solid contains Me_4NClO_4 as well as unidentified iron species.

Overall, these studies revealed that, while stable divalent metal ion complexes of the deprotonated amide bmppa$^-$ ligand can be formed for Ni^{II} and Co^{II}, an Fe^{II} analog cannot be generated under similar conditions.

Heating of 4 and 5 in Methanol

Heating of a methanol solution of the (deprotonated amide)Ni^{II} complex **4** at 50 °C for 5 d, followed by removal of the Ni^{II} ion using aqueous Na_2EDTA, produced the unaltered bmppa ligand in quantitative yield. Thus, complex **4**, which contains a deprotonated amide moiety akin to that found in [(bmppa$^-$)Zn]ClO_4,[17] does not undergo amide methanolysis. A rationale for the difference in reactivity between **4** and [(bmppa$^-$)Zn]ClO_4 involves the location of an anion binding site on the metal center. For the (deprotonated amide)Ni^{II} complex, reaction with methanol could produce a pseudo-octahedral complex, wherein the methoxide is in the same plane with the coordinated amide (Figure 7). This orientation would not be productive for intramolecular amide cleavage. For the zinc derivative, we have previously proposed that the reactive species involves a tri-

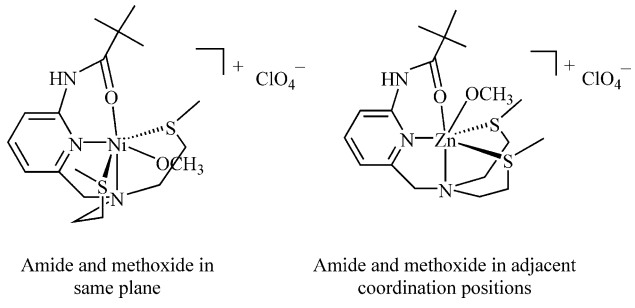

Figure 7. Proposed orientation of amide and methoxide anion in Ni^{II} and Zn^{II} complexes of the bmppa ligand.

gonal-prismatic structure, wherein the coordinated methoxide nucleophile and amide are in adjacent coordination positions (Figure 7).[17]

Heating of a methanol solution of the deprotonated amide complex **5** at 50 °C for 5 d under nitrogen, followed by removal of the Co^{II} ion using aqueous Na_2EDTA produced the amide methanolysis product bmapa {*N*,*N*-bis(2-methylthio)ethyl-*N*-[(6-amino-2-pyridyl)methyl]amine} in ca. 50% yield, along with unaltered bmppa ligand (ca. 43%), and a third product, *N*-(6-formylpyridin-2-yl)-2,2-dimethylpropanamide (ca. 7%).[21] The other amide methanolysis product (methyl trimethylacetate) is volatile and was not isolated or quantified. We attribute the formation of the aldehyde product to the presence of a trace amount of O_2 in the reaction mixture. Cobalt(II) complexes have been previously shown to undergo reaction with O_2 to generate reactive Co^{III} peroxide or hydroperoxide complexes that mediate the *N*-dealkylation of supporting chelate ligands.[23] The production of only ca. 50% of the chelate ligand amide methanolysis product after 5 d at 50 °C contrasts with the reactivity of the zinc analog [(bmppa$^-$)Zn]-ClO_4, wherein a 96% yield of bmapa is obtained after heating of the complex in methanol at 40(1) °C for 48 h and removal of the Zn^{II} ion. Note that control reactions have demonstrated that the bmppa ligand is unreactive in the absence of a metal ion.[16] On the basis of the structure of **2**, we speculate that a six-coordinate cobalt methoxide species may adopt either of the two structural types shown in Figure 7. If the thermodynamically more stable form is the pseudo-octahedral complex, it may rearrange with increased temperature to produce a pseudo-trigonal-prismatic geometry that is the reactive species for intramolecular amide methanolysis. Of relevance to this chemistry, we note that a trigonal-prismatic type of geometry, as is proposed for the Zn^{II} cation shown in Figure 7, has been previously identified in cadmium and mercury "parent" complexes of the bmppa and beppa {*N*,*N*-bis(2-ethylthio)ethyl-*N*-[(6-pivaloylamido-2-pyridyl)methyl]amine} ligands.[16,24] These complexes undergo methanolysis of the amide when treated with 1 equiv. of base in methanol-containing solutions. In the crystal structures of the Cd^{II} and Hg^{II} complexes a perchlorate anion is coordinated to the metal center (Figure 8). This perchlorate interaction produces an overall distorted trigonal-prismatic geometry at the metal center. We propose that the $-OCD_3$ nucleophile (Figure 7) interacts with the metal center in a similar fashion.

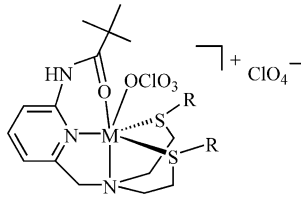

Figure 8. Structural features of cadmium and mercury "parent" complexes of amide-appended N_2S_2 ligands.

Conclusions

Divalent nickel, cobalt and iron complexes of the amide-appended N_2S_2 donor ligand bmppa have been isolated and characterized. These "parent" complexes exhibit distorted octahedral structures and amide oxygen coordination. In the presence of base, the Ni^{II} and Co^{II} complexes undergo reaction to yield isolable deprotonated amide complexes that have been characterized by multiple methods. Heating of methanol solutions of these deprotonated amide complexes produces amide cleavage products only in the case of the Co^{II} derivative. Notably, the reaction involving the Co^{II} complex is slower than the corresponding reaction involving a zinc analog. We propose that this difference is due to the reactive zinc complex exclusively adopting a distorted trigonal-prismatic geometry, whereas the Co^{II} analog may also adopt an unreactive distorted octahedral geometry. These results demonstrate the important role of metal coordination geometry preferences in influencing amide cleavage reactivity.

Experimental Section

General Remarks: Reagents and solvents were purchased from commercial sources and were used as received unless otherwise noted. Solvents for glove-box use were dried according to published procedures and were degassed prior to use.[25] FTIR spectra were recorded with a Shimadzu FTIR-8400 spectrometer as KBr pellets or as CH_3CN solutions (100 mM). ^1H and/or {^1H,^1H} COSY NMR spectra of paramagnetic Ni^{II}, Co^{II}, and Fe^{II} complexes were recorded in dry CD_3CN with a Bruker ARX-400 spectrometer. Chemical shifts (in ppm) are referenced to the residual solvent peak in CD_3CN [^1H: δ = 1.94 (quint) ppm]. The chelate ligand bmppa {*N*,*N*-bis(2-methylthio)ethyl-*N*-[(6-pivaloylamido-2-pyridyl)methyl]amine} was prepared as previously reported.[26] ***Caution!*** Perchlorate salts of metal complexes with organic ligands are potentially explosive. These compounds should be handled in small quantities and with extreme caution, especially in the solid state.[27]

[(bmppa)Ni(CH_3CN)](ClO_4)$_2$ (1): $Ni(ClO_4)_2{\cdot}6H_2O$ (0.0395 g, 0.108 mmol) dissolved in methanol (2 mL) was added to a solution of bmppa (0.0384 g, 0.108 mmol) in methanol (2 mL). The resulting purple solution was stirred at room temperature for ca. 30 min. Addition of excess of diethyl ether (ca. 60 mL) to the reaction mixture, followed by cooling at –15 °C for ca. 12 h resulted in the deposition of a purple precipitate, which was isolated and dried under vacuum. Recrystalization of this purple powder by diethyl ether diffusion into CH_3CN/CH_3OH (1:1) at ambient temperature yielded purple needle crystals (0.050 g, 70%). FTIR (KBr): $\tilde{\nu}$ = 3336 (ν_{N-H}), 1649, 1617, 1530, 1457, 1427, 1169, 1103, 1080 (ν_{ClO4}), 796, 623 (ν_{ClO4}) cm^{-1}. FTIR (CH_3CN, 100 mM, 1700–1550 cm^{-1} region): $\tilde{\nu}$ = 1653, 1620 cm^{-1}. $C_{19}H_{32}Cl_2N_4NiO_9S_2$ (652.03): calcd. C 34.97, H 4.95, N 8.59; found C 35.15, H 4.95, N 8.65.

[(bmppa)Co(CH_3CN)](ClO_4)$_2$ (2): This complex was prepared in an identical manner to **1**. Deep pink blocks suitable for X-ray diffraction studies were obtained from CH_3CN/Et_2O (0.044 g, 65%). FTIR (KBr): $\tilde{\nu}$ = 3318 (ν_{N-H}), 1635, 1612, 1528, 1452, 1422, 1099 (ν_{ClO4}), 791, 619 (ν_{ClO4}) cm^{-1}. FTIR (CH_3CN, 100 mM, 1700–1550 cm^{-1} region): $\tilde{\nu}$ = 1653, 1648, 1619 cm^{-1}. $C_{19}H_{32}Cl_2CoN_4O_9S_2$ (653.03): calcd. C 34.91, H 4.94, N 8.58; found C 34.89, H 4.83, N 8.36.

[(bmppa)Fe(CH_3CN)](ClO_4)$_2$ (3): Prepared in an identical manner to **1**. Recrystalization of the initially isolated yellow solid from CH_3CN/Et_2O yielded green needle crystals suitable for single-crystal X-ray diffraction (0.043 g, 65%). FTIR (KBr): $\tilde{\nu}$ = 3325 (br., ν_{N-H}), 1633, 1612, 1531, 1455, 1428, 1081 (ν_{ClO4}), 796, 623 (ν_{ClO4}) cm^{-1}. FTIR (CH_3CN, 100 mM, 1700–1550 cm^{-1} region): $\tilde{\nu}$ = 1636, 1619 cm^{-1}. $C_{19}H_{32}Cl_2FeN_4O_9S_2$ (650.03): calcd. C 35.08, H 4.96, N 8.62; found C 34.82, H 4.95, N 8.60.

[(bmppa$^-$)Ni]ClO_4 (4): $Me_4NOH\cdot5H_2O$ (0.022 g, 0.12 mmol) dissolved in methanol (2 mL) was added to a solution of **1** (0.080 g, 0.12 mmol) in acetonitrile (3 mL). The purple solution turned a light purple/lavender color upon the addition of the base. The resulting reaction mixture was stirred under nitrogen for ca. 4 h. The solvent was then evaporated under reduced pressure. The remaining solid was dissolved in CH_2Cl_2 and filtered through a Celite/glass wool plug. The filtrate was concentrated under vacuum to obtain a pale purple oil. This purple oil was dissolved in a minimal amount of methanol, and the product was precipitated using an excess of diethyl ether. Upon cooling to –15 °C for ca. 48–72 h, flaky purple crystals were formed in the solution. The solvent was decanted and the product dried under reduced pressure (0.017 g, 28%). FTIR (KBr): $\tilde{\nu}$ = 3400 (ν_{O-H}), 1618, 1605, 1567, 1489, 1447, 1419, 1107 (ν_{ClO4}), 911, 805, 623 (ν_{ClO4}) cm^{-1}. $C_{17}H_{28}ClN_3NiO_5S_2$ (512.69): calcd. C 39.92, H 5.52, N 8.22; found C 39.65, H 5.94, N 8.40.

[(bmppa$^-$)Co]$ClO_4\cdot H_2O$ (5): $Me_4NOH\cdot5H_2O$ (0.036 g, 0.20 mmol) dissolved in methanol (2 mL) was added to a solution of **2** (0.13 g, 0.20 mmol) in methanol (3 mL) . The red solution of the cobalt complex turned dark brown upon addition of the base. The resulting reaction mixture was stirred under nitrogen for ca. 6 h. The solvent was then evaporated under reduced pressure. The remaining solid was dissolved in CH_2Cl_2 and filtered through a Celite/glass wool plug, The filtrate was concentrated under vacuum to obtain a dark brown oil. This brown oil was dissolved in a minimal amount of acetonitrile and the product precipitated using excess diethyl ether. Upon cooling at –15 °C for 48 h, small dark brown crystals were formed in the solution. The solvent was decanted off and the product dried under reduced pressure to obtain a dark brown powder (0.066 g, 64%). FTIR (KBr): $\tilde{\nu}$ = 3433 (br., ν_{O-H}), 1653, 1617, 1570, 1559, 1457, 1419, 1101 (br., ν_{ClO4}), 806, 624 (ν_{ClO4}) cm^{-1}. $C_{17}H_{28}ClCoN_3O_5S_2$ (512.93): calcd. C 39.84, H 5.51, N 8.20; found C 38.21, H 5.28, N 8.19. Trace H_2O (ca. 1.0 equiv.) was present in the elemental analysis sample as indicated by an FTIR spectrum. Inclusion of this water in the calculated values produced a more satisfactory fit to the experimentally determined data. $C_{17}H_{28}N_3O_5S_2ClCo\cdot H_2O$ (530.06): calcd. C 38.49, H 5.70, N 7.93; found C 38.21, H 5.28, N 8.19.

Reaction of 3 with $Me_4NOH\cdot5H_2O$: $Fe(ClO_4)_2\cdot6H_2O$ (0.077 g, 0.22 mmol) dissolved in methanol (ca. 2 mL) was added to a solution of bmppa (0.077 g, 0.22 mmol) in methanol (ca. 2 mL). The resulting yellow solution was stirred under nitrogen for ca. 30 min. To this solution was added $Me_4NOH\cdot5H_2O$ (0.039 g, 0.22 mmol) dissolved in methanol (ca. 2 mL). This addition resulted in the immediate deposition of a green precipitate. The reaction mixture was stirred overnight, after which time the solvent was removed under reduced pressure, which yielded a yellow-green solid. Addition of CH_2Cl_2 produced a yellow solution, which was carefully transferred to another flask, and the remaining green solid was dried under vacuum. The green solid was washed with diethyl ether (3 × 2 mL), and the wash solutions were combined with the CH_2Cl_2 fraction and dried, which left a viscous yellow oil. The ^{1}H NMR features of this oil are consistent with those of the bmppa ligand (0.060 g, 78%). The green solid contains Me_4NClO_4, as determined by IR spectroscopy, and unidentified iron species.

Heating of 4 in MeOH: $Me_4NOH\cdot5H_2O$ (0.03 g, 0.16 mmol) dissolved in methanol (5 mL) was added to a solution of **1** (0.11 g, 0.16 mmol) in methanol (15 mL) and acetonitrile (5 mL). This produced a color change from purple to reddish purple, consistent with the formation of **4**. The reaction mixture was then heated at 50 °C under nitrogen for 5 d. After cooling to room temperature, Na_2EDTA (0.12 g, 0.33 mmol) dissolved in water (15 mL) was added. The pH of the solution was adjusted to 11 with aqueous NaOH, and the solution was stirred at room temperature for ca. 2 h. This aqueous solution was then extracted with CH_2Cl_2 (3 × 50 mL). The organic fractions were combined, dried with Na_2SO_4, and the solvents evaporated to dryness, which resulted in the isolation of a yellow oily product. ^{1}H NMR analysis of this oil indicated the isolation of unaltered bmppa ligand in quantitative yield.

Heating of 5 in MeOH: Complex **2** was generated in situ by combining methanol/acetonitrile (ca. 1:1) solutions of $Co(ClO_4)_2\cdot6H_2O$ (0.099 g, 0.25 mmol) and bmppa (0.088 g, 0.25 mmol). The resulting red solution of **2** was stirred under nitrogen for ca. 30 min. To this solution $Me_4NOH\cdot5H_2O$ (0.049 g, 0.25 mmol) dissolved in methanol (5 mL) was added. This produced a color change from red to dark brown, consistent with the formation of **5**. The reaction mixture was stirred at 50 °C under nitrogen for 5 d. The reaction mixture was then cooled to room temperature and Na_2EDTA (0.65 g, 1.74 mmol) dissolved in water (ca. 15 mL) added. The pH of the solution was adjusted to 11 with aqueous NaOH and the resulting mixture stirred at room temperature for ca. 2 h. The solution was extracted with CH_2Cl_2. All the organic fractions were collected, dried with Na_2SO_4, and the solvents evaporated to dryness to yield a brown oil. The ^{1}H NMR spectrum of this brown oil indicated the formation of two major products and one minor product in the reaction mixture. The first major product was *N*,*N*-bis-2-(methylthio)ethyl-*N*-[(6-amino-2-pyridyl)methyl]amine (bmapa) (ca. 50%). The second major product was unaltered bmppa ligand (43%). The third minor product obtained was *N*-(6-formylpyridin-2-yl)-2,2-dimethylpropanamide[22] (ca. 7%). ^{1}H NMR (CD_3CN, 400 MHz): δ = 9.87 (s, 1 H), 8.5 (br., NH), 8.41 (d, 1 H), 7.95 (t, 1 H), 7.66 (d, 1 H), 1.28 (s, 9 H) ppm. GC-MS: *m*/*z* (%) = 206 (9) $[M + H]^+$.

X-ray Crystallography: Single crystals of **2** and **3** were mounted on glass fibers with traces of viscous oil and then transferred to a NoniusKappaCD diffractometer with Mo-K_α radiation (λ = 0.71073 Å) for data collection at 200(1) K. Ten frames of data were collected with an oscillation range of 1 °/frame and an exposure time of 20 s/frame. Indexing and unit-cell refinement based on all observed reflections from those ten frames indicated a monoclinic *P* lattice for both complexes. A total of 16639 reflections for **2** and 11278 reflections for **3** were indexed, integrated, and corrected for Lorentz, polarization and absorption effects using DENZO-SMN and SCALEPAC.[28] The structures were solved by a combination of direct and heavy-atom methods using SIR 97.[29] All non-hydrogen atoms were refined with anisotropic displacement coefficients. For **2** all hydrogen atoms except the amide hydrogen atom were assigned isotropic displacement coefficients U(H) = 1.2 U(*C*) or 1.5 $U(C_{methyl})$ and their coordinates were allowed to ride on their respective carbon atoms using SHELXL97.[30] The amide hydrogen atom of **2** and all the hydrogen atoms of **3** were located and refined independently. Complexes **2** and **3** crystallized in the space group $P2_1/c$. Additional details of the X-ray data collection and refinement are given in Table 4. CCDC-648591 (for **2**), and -648592 (for

3) contain the supplementary crystallographic data for this paper. These data can be obtained free of charge from the The Cambridge Crystallographic Data Centre via www.ccdc.cam.ac.uk/data_request/cif.

Table 4. Summary of X-ray data collection and refinement.[a]

	2	**3**
Empirical formula	$C_{19}H_{32}Cl_2CoN_4O_9S_2$	$C_{19}H_{32}Cl_2FeN_4O_9S_2$
Formula mass	654.44	651.36
Crystal system	monoclinic	monoclinic
Space group	$P2_1/c$	$P2_1/c$
a [Å]	18.4261(7)	18.3663(3)
b [Å]	7.81940(10)	7.8281(1)
c [Å]	20.7120(8)	20.5577(4)
α [°]	90.0	90.0
β [°]	111.9960(11)	112.242(1)
γ [°]	90.0	90.0
V [Å^3]	2766.99(15)	2735.73(8)
Z	4	4
Density (calcd.) [Mg·m^{-3}]	1.571	1.581
T [K]	200(1)	200(1)
Crystal size [mm]	$0.30 \times 0.23 \times 0.15$	$0.25 \times 0.21 \times 0.11$
Diffractometer	Nonius KappaCCD	Nonius KappaCCD
Absorption coefficient [mm^{-1}]	1.018	0.953
$2\theta_{max}$ [°]	67.44	54.96
Completeness to 2θ (%)	85.7	99.3
Reflections collected	16639	11278
Independent reflections	9472	6227
Variable parameters	339	462
$R1/wR_2$[b]	0.0481/0.1182	0.0498/0.1155
Goodness-of-fit (F^2)	1.030	1.029
Largest difference [e Å^{-3}]	0.854/–0.474	1.047/–0.864

[a] Radiation used: Mo-K_α (λ = 0.71073 Å). [b] $R1 = \sum ||F_o| - |F_c|| / \sum |F_o|$; $wR_2 = \{\sum[w(F_o^2 - F_c^2)^2] / [\sum (F_o^2)^2]\}^{1/2}$ where $w = 1/[\sigma^2(F_o^2) + (aP)^2 + bP]$.

Acknowledgments

We thank the National Science Foundation (CAREER Award CHE-0094066) for funding of this research.

[1] P. T. R. Rajagopalan, X. C. Yu, D. Pei, *J. Am. Chem. Soc.* **1997**, *119*, 12418–12419.
[2] D. Groche, A. Becker, I. Schlichting, W. Kabsch, S. Schultz, A. F. V. Wagner, *Biochem. Biophys. Res. Commun.* **1998**, *246*, 342–346.
[3] A. Becker, I. Schlichting, W. Kabsch, D. Groche, S. Schultz, A. F. V. Wagner, *Nat. Struct. Biol.* **1998**, *5*, 1053–1058.
[4] E. T. Baldwin, M. S. Harris, A. W. Yem, C. L. Wolfe, A. F. Vosters, K. A. Currty, R. W. Murray, J. H. Bock, V. P. Marshall, J. I. Cialdella, M. H. Merchant, G. Choi, M. R. Deibel Jr, *J. Biol. Chem.* **2002**, *277*, 31163–31171.
[5] A. Becker, I. Schlichting, W. Kabsch, S. Schultz, A. F. Wagner, *J. Biol. Chem.* **1998**, *273*, 11413–11416.
[6] P. T. Rajagopalan, S. Grimme, D. Pei, *Biochemistry* **2000**, *39*, 779–790.
[7] S. Ragusa, S. Blanquet, T. Meinnel, *J. Mol. Biol.* **1998**, *280*, 515–523.
[8] F. Dardel, S. Ragusa, C. Lazennec, S. Blanquet, T. Meinnel, *J. Mol. Biol.* **1998**, *280*, 501–513.
[9] P. T. R. Rajagopalan, A. Datta, D. Pei, *Biochemistry* **1997**, *36*, 13910–13918.
[10] S. Chang, R. D. Sommer, A. l. Rheingold, D. P. Goldberg, *Chem. Commun.* **2001**, 2396–2397.
[11] S. Chang, V. V. Karambelkar, R. D. Sommer, A. L. Rheingold, D. P. Goldberg, *Inorg. Chem.* **2002**, *41*, 239–248.
[12] R. C. diTargiani, S. Chang, M. H. Salter, R. D. Hancock, D. P. Goldberg, *Inorg. Chem.* **2003**, *42*, 5825–5836.
[13] D. P. Goldberg, R. C. diTargiani, F. Namuswe, E. C. Minnihan, S. Chang, L. N. Zakharov, A. L. Rheingold, *Inorg. Chem.* **2005**, *44*, 7559–7569.
[14] V. V. Karambelkar, C. Xiao, Y. Zhang, A. A. Sarjeant, D. P. Goldberg, *Inorg. Chem.* **2006**, *45*, 1409–1411.
[15] R. A. Allred, K. Doyle, A. M. Arif, L. M. Berreau, *Inorg. Chem.* **2006**, *45*, 4097–4108.
[16] L. M. Berreau, M. M. Makowska-Grzyska, A. M. Arif, *Inorg. Chem.* **2000**, *39*, 4390–4391.
[17] E. Szajna, M. M. Makowska-Grzyska, C. C. Wasden, A. M. Arif, L. M. Berreau, *Inorg. Chem.* **2005**, *44*, 7595–7605.
[18] G. K. Ingle, M. M. Makowska-Grzyska, E. Szajna-Fuller, I. Sen, J. C. Price, A. M. Arif, L. M. Berreau, *Inorg. Chem.* **2007**, *46*, 1471–1480.
[19] D. R. McMillin in *Physical Methods in Bioinorganic Chemistry: Spectroscopy and Magnetism* (Ed.: L. Que Jr,), University Science Books, Sausalito, CA, **2000**, pp. 1–58.
[20] D. F. Evans, *J. Chem. Soc.* **1959**, 2003–2005.
[21] W. L. Jolly, *The Synthesis and Characterization of Inorganic Compounds*, Waveland Press, Inc., Prospect Heights, IL, **1970**.
[22] T. Mase, I. N. Houpis, A. Akao, I. Dorziotis, K. Emerson, T. Hoang, T. Iida, T. Itoh, K. Kamei, S. Kato, Y. Kato, M. Kawasaki, F. Lang, J. Lee, J. Lynch, P. Mailgres, A. Molina, T. Nemoto, S. Okada, R. Reamer, J. Z. Song, D. Tschaen, T. Wada, D. Zewge, R. P. Volante, P. J. Reider, K. Tomimoto, *J. Org. Chem.* **2001**, *66*, 6775–6786.
[23] P. Comba, S. Kuwata, G. Linti, H. Prizkow, M. Tarnai, H. Wadepohl, *Chem. Commun.* **2006**, 2074–2076 and references cited therein.
[24] M. M. Makowska-Grzyska, K. Doyle, R. A. Allred, A. M. Arif, D. C. Bebout, L. M. Berreau, *Eur. J. Inorg. Chem.* **2005**, 822–827.
[25] W. L. F. Armarego, D. D. Perrin, *Purification of Laboratory Chemicals*, 4th ed., Butterworth-Heinemann, Boston, MA, **1996**.
[26] L. M. Berreau, R. A. Allred, M. M. Makowska-Grzyska, A. M. Arif, *Chem. Commun.* **2000**, 1423–1424.
[27] W. C. Wolsey, *J. Chem. Educ.* **1973**, *50*, A335–A337.
[28] Z. Otwinowski, M. Minor, *Methods Enzymol.* **1997**, *276*, 307–326.
[29] A. Altomare, M. C. Burla, M. Camalli, G. L. Cascarano, C. Giacovazzo, A. Guagliardi, A. G. G. Moliterni, G. Polidori, R. Spagna, *J. Appl. Crystallogr.* **1999**, *32*, 115–199.
[30] G. M. Sheldrick, *SHELXL-97, Program for the Refinement of Crystal Structures*, University of Göttingen, Germany, **1997**.

Received: June 5, 2007
Published Online: September 24, 2007

